chemosensors

IMPACT FACTOR 3.7

CITESCORE 5.0

Article

Ascorbic Acid Sensing by Molecularly Imprinted Electrosynthesized Polymer (e-MIP) on Screen-Printed Electrodes

Giancarla Alberti, Camilla Zanoni, Lisa Rita Magnaghi and Raffaela Biesuz

Special Issue

10th Anniversary of *Chemosensors*—Section 'Electrochemical Devices and Sensors'

Edited by

Prof. Dr. Edward P. C. Lai

MDPI

https://doi.org/10.3390/chemosensors11060348

chemosensors

Article

Ascorbic Acid Sensing by Molecularly Imprinted Electrosynthesized Polymer (e-MIP) on Screen-Printed Electrodes

Giancarla Alberti [1,*], Camilla Zanoni [1], Lisa Rita Magnaghi [1,2] and Raffaela Biesuz [1,2]

[1] Department of Chemistry, University of Pavia, Via Taramelli 12, 27100 Pavia, Italy; camilla.zanoni01@universitadipavia.it (C.Z.); lisarita.magnaghi@unipv.it (L.R.M.); rbiesuz@unipv.it (R.B.)
[2] Unità di Ricerca di Pavia, Consorzio Interuniversitario Nazionale per la Scienza e Tecnologia dei Materiali (INSTM), Via G. Giusti 9, 50121 Firenze, Italy
* Correspondence: galberti@unipv.it

Abstract: This paper presents the development of a cheap and rapid electrochemical sensor for ascorbic acid detection. In particular, the graphite ink working electrode of screen-printed cells was covered by a film of elecrosynthesized molecularly imprinted polypyrrole (e-MIP); differential pulse voltammetry (DPV) was the selected method for the analyte detection. The ascorbic acid molecules were successfully entrapped in the polypyrrole film, creating the recognition sites. The best results were obtained after polypyrrole overoxidation and performing the measurements in phosphate buffer solution 0.05 M/KCl 0.1 M at pH 7.5. A comparison with the bare and the not-imprinted polypyrrole-modified electrodes showed that the e-MIP-based sensor had the highest selectivity and reproducibility. The developed method was applied to assess ascorbic acid in farmaceutical products, obtaining values not significantly different from the declared content.

Keywords: ascorbic acid; electrosinthesized molecularly imprinted polymers; molecularly imprinted polypyrrole; screen-printed electrodes; voltammetric sensors; chemosensors; analytical chemistry

Citation: Alberti, G.; Zanoni, C.; Magnaghi, L.R.; Biesuz, R. Ascorbic Acid Sensing by Molecularly Imprinted Electrosynthesized Polymer (e-MIP) on Screen-Printed Electrodes. *Chemosensors* **2023**, *11*, 348. https://doi.org/10.3390/chemosensors11060348

Academic Editor: Pi-Guey Su

Received: 12 May 2023
Revised: 8 June 2023
Accepted: 14 June 2023
Published: 16 June 2023

1. Introduction

The L enantiomer of ascorbic acid (AA), also named vitamin C, is a hydrosoluble vitamin with well-established antioxidant properties [1]. In fact, all its known physiological and biochemical actions are due to its behavior as an electron donor, i.e., a reducing agent [1–4]. Ascorbic acid can be found in many biological systems and foods, such as fresh vegetables, fruits, and legumes. It is involved in collagen synthesis, iron absorption, and immune response activation. Moreover, vitamin C participates in osteogenesis and wound healing; it helps maintain bones, teeth, and capillaries [2–4].

By contrast, ascorbic acid excess can cause gastric irritations, and its metabolite, oxalic acid, provokes renal problems. Under certain circumstances, excessive quantities of vitamin C can induce inhibition of natural processes occurring in food, contributing to aroma and taste deterioration [1].

Ascorbic acid quickly degrades in the presence of some enzymes and atmospheric oxygen; its oxidation is also promoted by excessive light, heat, and heavy metal ions [1]. It is commonly used as an antioxidant in the foodstuff industry to inhibit undesired changes in flavor or color. Its antioxidant properties make it an important quality indicator for foods and drinks [5–7].

Given the crucial role of vitamin C in biochemistry and industrial purposes, monitoring ascorbic acid concentration during food and drug production and quality control analysis using rapid, sensitive, and selective methods is very important [1,8].

Old classical methods for ascorbic acid detection include redox titrations with oxidants such as potassium iodate or bromate and dichlorophenol indophenol [9,10]. HPLC

techniques with amperometric or fluorimetric detection were employed for ascorbic acid determination in food and biological samples [11–13]. Spectrophotometric and fluorimetric methods were also frequently applied [14–18]. Significant progress has also been made in developing electrochemical sensors for ascorbic acid detection [19–27]. Compared to bulky and expensive instruments, electrochemical methods are often preferred thanks to the simplicity of the procedures, minimum sample pretreatment, fast response, reasonable sensitivity, and low cost. The direct electrochemical methods for ascorbic acid detection, exploiting its irreversible oxidation reaction to dehydroascorbic acid, have suffered from poor reproducibility and fouling of the electrode surface; moreover, interferences from electroactive substances often present in biological fluids or drugs, for example, dopamine and uric acid, make these methods ineffective [28,29]. Several strategies were proposed to overcome these drawbacks by chemically modifying the surfaces of the electrodes [30–36]. Despite the unquestionable good figures of merit in terms of sensitivity and detection limits, the need for lengthy and multi-step functionalization procedures, sometimes the synthesis of the immobilized receptor, and the use of delicate noble metal electrodes that require deep cleaning prevent their applicability to routine analysis and in non-specialized laboratories. In other proposed sensors, the selectivity of the methods was improved by adopting molecular imprinting technology [37–40].

Molecularly imprinted polymers (MIPs) are crosslinked polymers synthesized in the presence of a target analyte used as a template molecule which, after extraction, leaves complementary cavities in the polymeric network. These cavities have functional groups in a "frozen" orientation/conformation that permits the specific recognition of the template. The rebinding of the target analyte by the MIP is highly selective since the artificial receptors are shaped by the template [41–43]. MIPs can be seen as synthetic receptors that, contrary to their natural counterparts, i.e., antibodies, are low-cost, chemically and thermally stable, can be stored at room temperature without degradation, and are not obtained from animals.

At present, electrochemical sensors are some of the most effectively used MIP-based devices [41–51], and different strategies have been proposed for integrating MIPs with the electrodes. Surface imprinting is, so far, the most commonly used approach. The deposition of a MIP layer directly on the electrode surface represents a suitable method for obtaining a thin film of the polymer. It can be easily performed by drop casting the pre-polymeric mixture onto the electrode surface, followed by thermal or UV polymerization [51]. Recently, several studies reported on the application of electrosynthesized MIPs (e-MIPs) for developing electrochemical sensors (see, for example, the interesting review of L.M. Gonçalves [52]). In fact, electropolymerization allows for highly controlled polymer growth on surfaces with a fine tuning of the polymeric film thickness by controlling experimental conditions [52–54]. Other electrochemical procedures can also be applied to enhance these e-MIPs. One of them, which is very useful, is overoxidation, performed by the electrochemical treatment of the MIP film by positive electrode potentials much higher than those required for the polymerization reaction. Overoxidation is advantageous in MIPs' preparation since it allows the formation of carboxyl, carbonyl, and hydroxy groups able to interact by hydrogen bonds with the template molecule, promoting the formation of more selective cavities [55].

The most frequently electropolymerized imprinted films are primary polypyrrole, followed by polyaniline and polythiophene derivatives [56]. The focus on polypyrrole is due to its water solubility and ease of oxidation; moreover, polypyrrole possesses several valuable characteristics, such as good environmental stability, conductivity, and redox properties [57]. When submitted to high positive potentials, it can be overoxidized, and the incorporation of carbonyl groups into the polymer's backbone occurs, causing a loss of electric conductivity but also the filling of pinholes and defects. At the same time, higher control of the film thickness arises, and the background currents are more stable [52,57–59].

In this context, an electrochemical sensor based on electrosynthesized polypyrrole, molecularly imprinted with ascorbic acid and overoxidated, was developed. The polymeric film was electrodeposited on the graphite working electrode of a screen-printed cell, obtain-

ing a selective and simple method for AA sensing. Differential pulse voltammetry (DPV) was selected for the analyte detection, and the electrochemical parameters were optimized by a Design of Experiments (DoE).

Interference tests and trials with drugs were performed to assess the selectivity and reliability of the proposed method.

Differently from previously proposed and similar e-MIP-based electrochemical sensors for this analyte [37–40], the highlighted advantages are the low cost of the electrodes and apparatus, reduced quantity of reagents both for the electrode surface modification and template removal, unnecessary sample pretreatment, rapid responses, and the possibility to perform analyses in situ thanks to a portable instrument. The analytical figures of merit of the method are comparable to those of the previously proposed sensors (see Table 1). Moreover, the stability of the current signal and the reproducibility of the measurements were achieved thanks to the polypyrrole overoxidation allowing the reuse of disposable screen-printed cells for 3–5 analyses without loss of performance.

Table 1. Comparison of the figures of merits of the molecularly imprinted polypyrrole-based electrodes for ascorbic acid detection.

Electrode	Method	Linear Range (μM)	LOD (μM)	Ref.
PPy-MIP/ISE [1]	potentiometry	5–2000	3	[37]
Poly(Py-oPD)-MIP/PGE [2]	SWV [6]	1–1000	0.26	[38]
PPy-MIP/PGE [3]	DPV [7]	250–7000	74	[39]
PPy-EG-MIP/GCE [4]	DPV [7]	500–8000	100	[40]
PPy-MIP/SPC [5]	DPV [7]	30–2400 [8] 2–100 [9]	21 [8] 1.2 [9]	This work

[1] PPy-MIP/ISE = ion-selective electrode with molecularly imprinted polypyrrole membrane. [2] Poly(Py-oPD)-MIP/PGE = molecularly imprinted copolymer of pyrrole and o-phenylenediamine on a pencil graphite electrode. [3] PPy-MIP/PGE = molecularly imprinted polypyrrole on a pencil graphite electrode. [4] PPy-EG-MIP/GCE = molecularly imprinted polypyrrole-exfoliated graphene-modified glassy carbon electrode. [5] PPy-MIP-SPC = molecularly imprinted polypyrrole on the graphite-ink working electrode of a screen-printed cell. [6] SWV = square wave voltammetry. [7] DPV = differential pulse voltammetry. [8] calibration in 10 mL of solution. [9] calibration in 100 mL of solution.

2. Materials and Methods

2.1. Reagents and Instruments

Pyrrole (98%, Merk Life Science S.r.l., Milan, Italy) was distilled by a Hickman distillation head until a colorless liquid was obtained and kept in darkness at 4 °C. Lithium perchlorate ($LiClO_4$, purum p.a., ≥98.0%, Merk Life Science S.r.l., Milan, Italy), potassium dihydrogen phosphate (KH_2PO_4, ACS reagent, ≥99.0%, Merk Life Science S.r.l., Milan, Italy), and L-Ascorbic acid (analytical standard, Supelco—Merk Life Science S.r.l., Milan, Italy) were used as well as received. Phosphate buffer solutions (PBS) were prepared in double-distilled water, moving the pH to the desired value with HCl or NaOH standardized solutions (Merk Life Science S.r.l., Milan, Italy). Solutions of potassium chloride, potassium hexacyanoferrate(III), and sodium chloride (Merk Life Science S.r.l., Milan, Italy) were employed for electrodes' surface characterization. VIVIN C® tablets (Menarini Industrie Farmaceutiche Riunite S.r.l., Firenze, Italy) and TIOBEC® 400 tablets (Laborest, Milan, Italy) were purchased from a local pharmacy (Farmacia Fapa, Pavia, Italy).

Three-electrode screen-printed cells with graphite-ink working and counter electrodes and a Ag/AgCl-ink pseudo-reference electrode were obtained from Topflight Italia S.P.A. (Vidigulfo, Pavia, Italy).

Voltammetric and EIS (Electrochemical Impedance Spectroscopy) analyses were performed with the instrument EmStat4s (PalmSens BV, Houten, The Netherlands).

2.2. Preparation of the e-MIP and e-NIP Sensors

Before modification, each screen-printed cell (SPC) was washed with ethanol and left to dry at room temperature under a hood.

The e-MIP-modified electrode was prepared by electrodeposition on the surface of the clean SPC using cyclic voltammetry (CV) in the potential range −0.6–0.8 V during five cycles (scan rate 0.1 V/s) in an aqueous solution of 0.1 M $LiClO_4$, 15 mM pyrrole, and 10 mM ascorbic acid. The polypyrrole-imprinted film was overoxidized by applying a fixed potential of +1.2 V for 2 min in 0.1 M $LiClO_4$ solution. The extraction of the template was performed in two steps. Firstly, the modified SPC was placed in PBS solution 0.05 M at pH 7.5 for 20 min, under gentle stirring on an orbital shaker, followed by 10–15 cycles of cyclic voltammetry, scanning the potential from −1 to +1 V (scan rate 0.1 V/s) in PBS solution 0.05M/KCl 0.1 M at pH = 7.5.

Electropolimerized, not-imprinted polymer films on the working electrode of the SPC (e-NIPs) were prepared under the same conditions but without adding the template, i.e., AA, in the polymerization solution.

2.3. Characterization of the Working Electrode Surface

The electrochemically active area was measured before and after the working electrode modification with e-MIP or e-NIP.

It was determined by cyclic voltammetry in an electrochemical probe solution (5 mM $K_4Fe(CN)_6$/0.1 M KCl solution at pH 7), scanning the potential from −1 to +1 V, varying the scan rate from 0.025 to 0.5 V/s.

The intensity of the anodic or cathodic peak was plotted vs. the square root of the scan rate, and from the slope (*K*) the effective area was computed by applying the modified Randles–Sevick's equation [60,61]:

$$A = \frac{K}{2.69 \cdot 10^5 \cdot n^{3/2} \cdot D^{1/2} \cdot C} \quad (1)$$

D is the diffusion coefficient ($3.09 \cdot 10^{-6}$ cm^2/s) and *C* is the concentration (5 mM) of the electrochemical probe $K_4Fe(CN)_6$; *n* is the number of the electrons acquired for the reduction of the electrochemical probe (in this case, *n* = 1).

The double-layer capacitance I of the working electrodes [61–63] before and after modification was determined by cyclic voltammetry in 0.1 M NaCl solution at different scan rates, scanning the potential from +0.05 to −0.05 V, i.e., in a potential interval by which non-faradic current is expected. The difference between the anodic and cathodic current at 0.02 V was plotted versus the scan rate, and the slope of the straight line obtained corresponds to the capacitance. Dividing this value by two, the capacitance of the double layer can be obtained.

Further characterization of the working electrode surface (before and after modification) was carried out by Electrochemical Impedance Spectroscopy (EIS), a widespread technique used to characterize the electrode surfaces and define the electrochemical processes that occur at an electrolyte–electrode interface [64]. By the EIS technique, the impedance of a system is measured in relation to ac potential frequency. The data obtained from the EIS measurements can be modeled by the Randles equivalent circuit, which associates different electrical components to electrochemical processes [65]; it does not accurately represent the chemical behavior of the electrode/solution interface but is helpful for a graphical representation of the system. The impedance results can be graphically represented by the Nyquist plot, in which the negative imaginary impedance −Z″ is plotted vs. the real part Z′. This plot is typically characterized by two trends: the first, at high frequencies, is a semicircle that represents the charge transfer processes occurring at the electrode/solution interface; from the diameter of this semicircle, the charge transfer resistance (R_{CT}) can be determined; the second part, at lower frequencies, is a straight line that characterizes the mass-diffusion-limited processes [65].

EIS measurements were here performed for the bare and modified electrodes using 10 mL of $K_4Fe(CN)_6$ 5 mM and KCl 0.1 M at pH 7.5 as the probe solution. The impedance was registered in the frequency range of 100 kHz–10 mHz with a sinusoidal potential modulation of 0.05 V superimposed on a dc potential of 0.2 V.

2.4. Ascorbic Acid Determination by Differential Pulse Voltammetry (DPV)

Ascorbic acid was detected by differential pulse voltammetry (DPV) in 10 mL of 0.05 M PBS/0.1 M KCl solutions at pH 7.5, applying the following experimental conditions, optimized by a Design of Experiments (DoE) approach (described in Section 3.1): E_{start} = −0.5 V; E_{end} = 0.3 V; E_{step} = 0.01 V; E_{pulse} = 0.025 V; t_{pulse} = 0.25 s; scan rate = 0.02 V/s.

3. Results

3.1. Optimization of the DPV Method for Ascorbic Acid Detection

A full factorial design 2^3 was applied to optimize the following DPV parameters: pulse potential (E_p, V), pulse time (t_p, s), and scan rate (v, V/s). Preliminary considerations are essential before selecting the variable levels, and based on instrumental limits, the broadening of peaks, and the time of analysis, the experimental domain was selected.

Table 2 reports the minimum and maximum levels of the parameters under investigation. The slope of the three-point calibration curve was chosen as the response. The open-source software CAT (Chemometric Agile Tool) [66] was employed for data processing.

Table 2. Optimization of the DPV parameters by a full factorial design 2^3: level definitions for the parameters considered, keeping constant the range of the potential scan (from −0.5 V to +0.3 V).

Parameter	Minimum Level (−1)	Maximum Level (+1)
E_{pulse} (E_p, V)	0.015	0.025
t_{pulse} (t_p, s)	0.15	0.25
scan rate (v, V/s)	0.01	0.02

The bar graph of Figure 1 shows the significance of the model's coefficients, and their values are reported in Table 3.

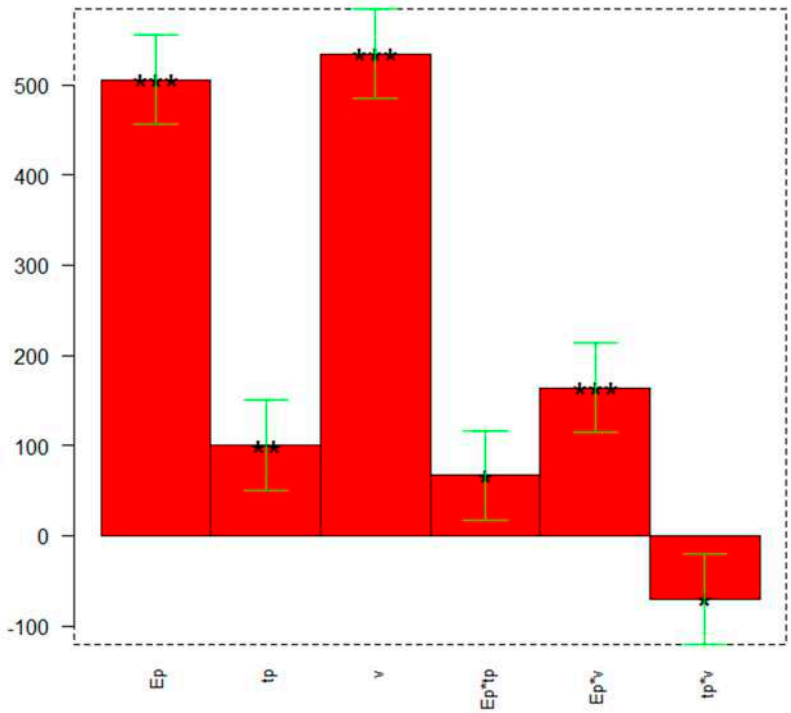

Figure 1. DoE to optimize the DPV parameters: coefficients plot. The greatest values and little black stars (irrespective of the sign) indicate a significant influence of the respective parameters or their interaction and significance (* $p \leq 0.05$, ** $p \leq 0.01$, *** $p \leq 0.001$).

Table 3. Optimization of the DPV parameters by a full factorial design 2^3: coefficient values and their significance (* $p \leq 0.05$, ** $p \leq 0.01$, *** $p \leq 0.001$).

Coefficient	Value	Significance
b_0	932	
b_1	505.74	***
b_2	100.13	**
b_3	534.08	***
b_{12}	66.96	*
b_{13}	164.07	***
b_{23}	−70.49	*

The following model equation can be expressed by

$$slope = b_0 + b_1 \cdot E_p + b_2 \cdot t_p + b_3 \cdot v + b_{12} \cdot E_p \cdot t_p + b_{13} \cdot E_p \cdot v + b_{23} \cdot t_p \cdot v \quad (2)$$

From the coefficients plot of Figure 1, it can be observed that all parameters are important and have a positive effect on the response, so they must be set at the maximum value (+1). The most significant interaction is between the pulse potential (E_p) and the scan rate (v), presenting a significant positive effect on the response.

Three replicates at the center point [0 0 0] were performed; Table 4 reports the average value, standard deviation, and confidence interval (CI) at a 95% confidence level. The model is validated since the predicted slope value fits into the CI.

Table 4. Optimization of the DPV parameters by a full factorial design 2^3: model validation by three replicates at the center point [0 0 0], i.e., E_p = 0.02 V; t_p = 0.2 s; v = 0.015 V/s. CI = confidence interval at 95% confidence level.

	Slope ($\mu A \cdot M^{-1}$)
Average	975
Standard deviation	49
Upper bound CI	1024
Lower bound CI	926
Predicted response (b_0)	932

Therefore, the optimal DPV parameters are pulse potential (E_p) 0.025V, pulse time (t_p) 0.25 s, and scan rate (v) 0.02 V/s.

3.2. Characterization of the Working Electrode Surface

The electrochemically active area and the double-layer capacitance were determined before and after the working electrode modification with e-MIP or e-NIP. Moreover, Electrochemical Impedance Spectroscopy (EIS) measurements were implemented to evaluate the electron transfer kinetics of the bare and modified electrodes.

The active area was obtained by cyclic voltammetric measurements in an electrochemical probe solution (here, $K_4Fe(CN)_6$) at different scan rates. The reduction or oxidation peak height was plotted against the square root of the scan rate, and the slope of the straight line (K) was entered into the Randles–Sevick equation (Equation (1), Section 2.3) to calculate the active area.

Since both oxidation and reduction peaks were measured, Table 5 shows the average of the two area values.

From Table 6, it can be observed that the active area decreases after coating the electrode with the polymer. As expected, the active area of the e-NIP-modified electrode is lower than that of the e-MIP. Indeed, the absence of the polymer's recognition cavities leads to a decrease in the electroactive surface.

Table 5. Active area values calculated by the Randles–Sevick equation. Electrochemical probe solution: 5 mM $K_4Fe(CN)_6$/0.1 M KCl, pH 7.5. Potential scan from −1 to +1 V; scan rate from 0.025 to 0.5 V/s.

	Active Area (mm^2) †
Bare electrode	3.8(2)
e-MIP-modified electrode	2.4(2)
e-NIP-modified electrode	1.3(1)
Geometric area (circular-shaped electrode ø 1.1 mm)	3.8

† mean values obtained by plotting both the cathodic and the anodic peaks vs. $(\text{scan rate})^{0.5}$; the number in parenthesis is the standard deviation of the last digit.

Regarding the double-layer capacitance, a value of 0.50(3) µF was obtained for the bare electrode, definitely low compared to that of glassy carbon electrodes. As previously reported, this can be ascribable to the different structure of the graphite ink of the screen-printed electrode employed here, with a predominance of basal planes compared to edge-plane pyrolytic graphite electrodes that exhibit faster electrochemical kinetics [59,67]. The double-layer capacitance increased from the bare electrode to the overoxidated e-NIP (1.52(6) µF) and e-MIP (2.15(5) µF) functionalized electrodes; this implies that the presence of the polymer layer increases the possibility of accumulating electrical charges.

The characterization of the bare and modified electrodes was also implemented by EIS measurements. Figure 2 shows the Nyquist plot (imaginary impedance $-Z''$ vs. real impedance Z') of bare and modified electrodes.

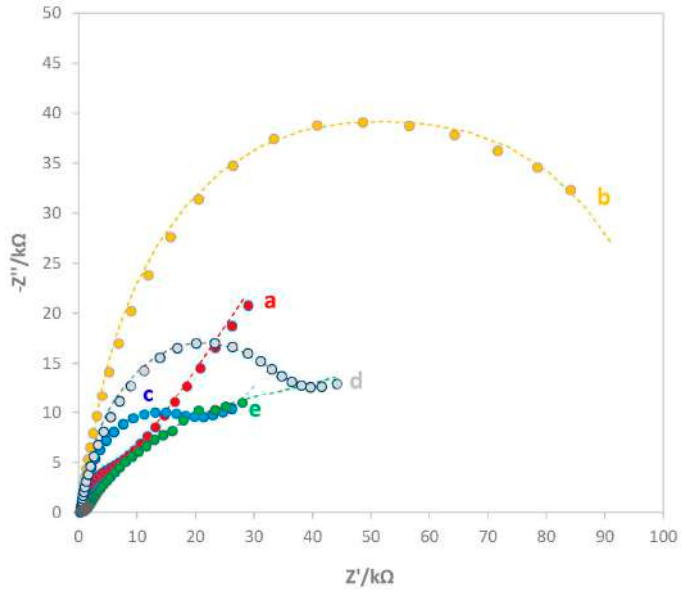

Figure 2. Nyquist plot of (**a**) bare electrode, (**b**) e-MIP-modified electrode, (**c**) e-MIP-modified electrode after template removal, (**d**) e-MIP-modified electrode after rebinding with AA 3 mM, (**e**) e-NIP-modified electrode. Measurements were performed in 5 mM $K_4Fe(CN)_6$/0.1 M KCl solution. Frequency range 100 kHz–10 mHz with a sinusoidal potential modulation of 0.05 V superimposed on a dc potential of 0.2 V.

As can be observed from Figure 2, the presence of the polymeric films influenced the impedance behavior of the electrode surface at both high- and low-frequency regions. The bare displayed the smallest R_{CT} (**a**), while the other electrodes modified with the overoxidate polypyrrole film showed a higher resistance to the charge transfer, indicating that by overoxidation, the conductive properties of polypyrrole were lost. The curves (**b**) and (**e**), i.e., the e-MIP before template removal and the e-NIP-modified electrodes, showed a similar behavior; indeed, the absence of a mass diffusion process due to the massive R_{CT} of the

uniform polymer films on the working electrode surface occurred. On the other hand, the curves (**c**), (**d**), and (**a**), corresponding, respectively, to the e-MIP-modified electrode after template removal, the same electrode after rebinding with 3 mM AA solution, and the bare electrode, have their working electrode surfaces more exposed to the solution; for this reason, the mass transfer diffusion processes is significant. The Randles circuits reported in Figure 3 schematize the two different trends. In both circuits, the element R corresponds to the solution resistance, R_{CT} is the electron transfer resistance (i.e., the diameter of the semicircle in the Nyquist plot), and C is the double-layer capacitance. The Randles circuit in Figure 2b is also described by a Warburg element representing the contribution of the mass-diffusion-limited process.

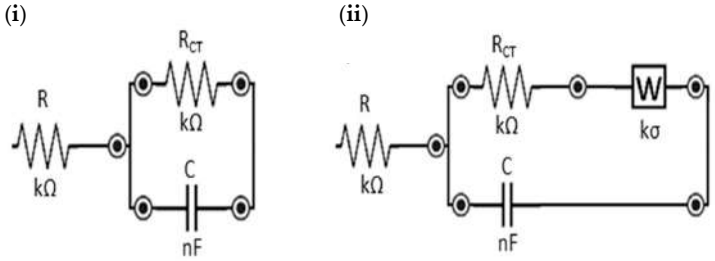

Figure 3. Randles equivalent circuit for modeling the Nyquist plots of Figure 2. (**i**) for bare (curve **a** in Figure 2) and e-NIP-modified electrodes (curve **e** in Figure 2); (**ii**) for e-MIP-modified electrode (curve **b** in Figure 2), e-MIP-modified electrode after template removal (curve **c** in Figure 2), e-MIP-modified electrode after rebinding with AA 3 mM (curve **d** in Figure 2).

The most significant parameter is R_{CT}: the higher the value, the more difficult the charge transfer. The R_{CT} for the e-MIP-modified electrode before template removal is about 50 kΩ higher than that of the e-NIP-modified electrode (45 kΩ); this behavior is probably due to the more porous structure of the e-NIP, which enables the electrochemical probe to reach the electrode surface a little easier. The R_{CT} values increase while the analyte occupies the recognition cavities of the e-MIP because the molecules make it harder for the ions to reach the electrode surface. The experimental data confirm this hypothesis: bare (curve **a** in Figure 2), R_{CT} 5.4 kΩ; e-MIP-modified electrode after removal of the template (curve **c** in Figure 2), R_{CT} 20 kΩ; e-MIP-modified electrode after rebinding with AA 3 mM (curve **d** in Figure 2), R_{CT} 22 kΩ.

3.3. Electropolymerization of Molecularly Imprinted Polypyrrole and Overoxidation

Electropolymerization of the pyrrole was performed via cyclic voltammetry in the potential range −0.6–0.8 V, at a scan rate 0.1 V/s, in an aqueous solution of 0.1 M $LiClO_4$, 15 mM pyrrole, and 10 mM ascorbic acid. Five scans were performed as a good compromise between a polymer film that is too thick with less accessible recognition sites [68], achievable with more than seven scans, and insufficient formation of the imprinted cavities with fewer scans.

Figure 4 shows the cyclic voltammograms recorded during the pyrrole's electropolymerization on the working electrode of the screen-printed cells without AA (Figure 4a) and with the template (Figure 4b).

During the e-NIP polymerization (see Figure 4a), a broad oxidation peak appeared at about −0.2 V and a reverse reduction peak at approximately 0 V; the intensity of both peaks increased as the polymeric film grew. In the presence of ascorbic acid, during the e-MIP synthesis (Figure 4b), an oxidation peak at 0.2 V appeared, indicating the incorporation of the template molecules into the polymeric chain formed on the working electrode. Indeed, ascorbic acid molecules diffusing toward the electrode surface during the electropolymerization process were trapped in the polymer network; the formation of the imprinting cavities was promoted by the diffusion of the electroactive analyte to the electrode surface, generating the recognition sites during the electrosynthesis of

the polypyrrole, as previously suggested [39,40,69–73]. As is well known, ascorbic acid undergoes oxidation to dehydroascorbic acid through an irreversible reaction [1], so only the anodic oxidation peak at about 0.4 V appears in CV scans of ascorbic acid solutions on a bare electrode (see Figure 5).

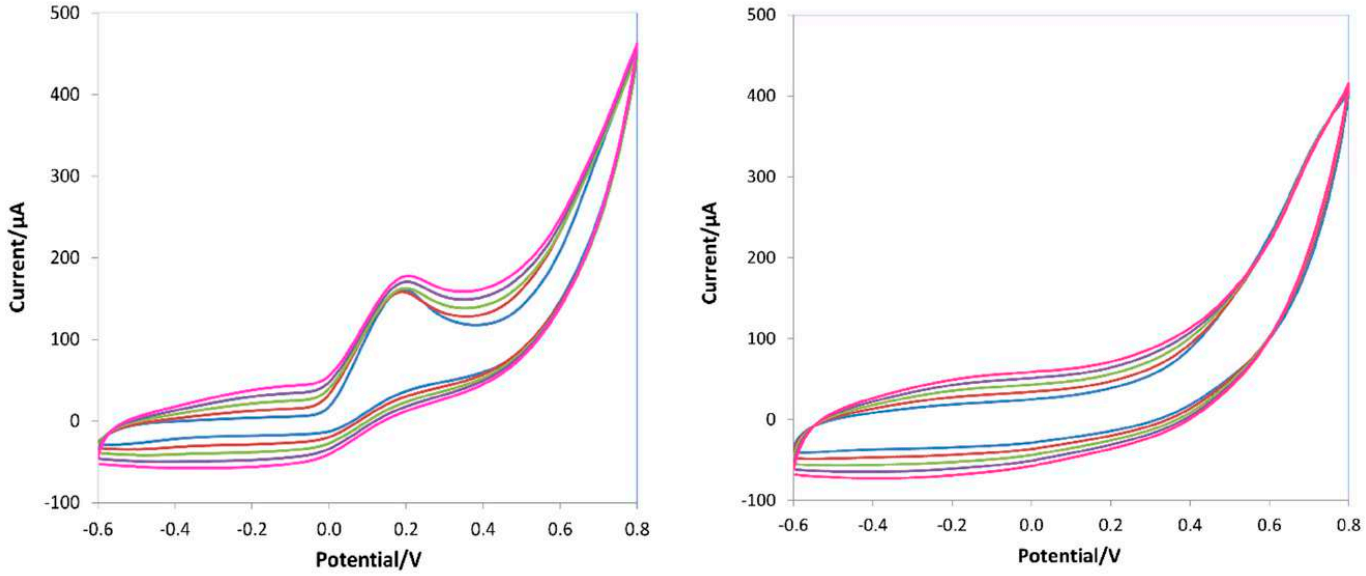

(**a**) (**b**)

Figure 4. Cyclic voltammograms during the electropolymerization of 15 mM pyrrole in 0.1 M $LiClO_4$ in the absence (**a**) and in the presence of 10 mM ascorbic acid (**b**). Potential range −0.6–0.8 V, scan rate 0.1 V/s, five scans.

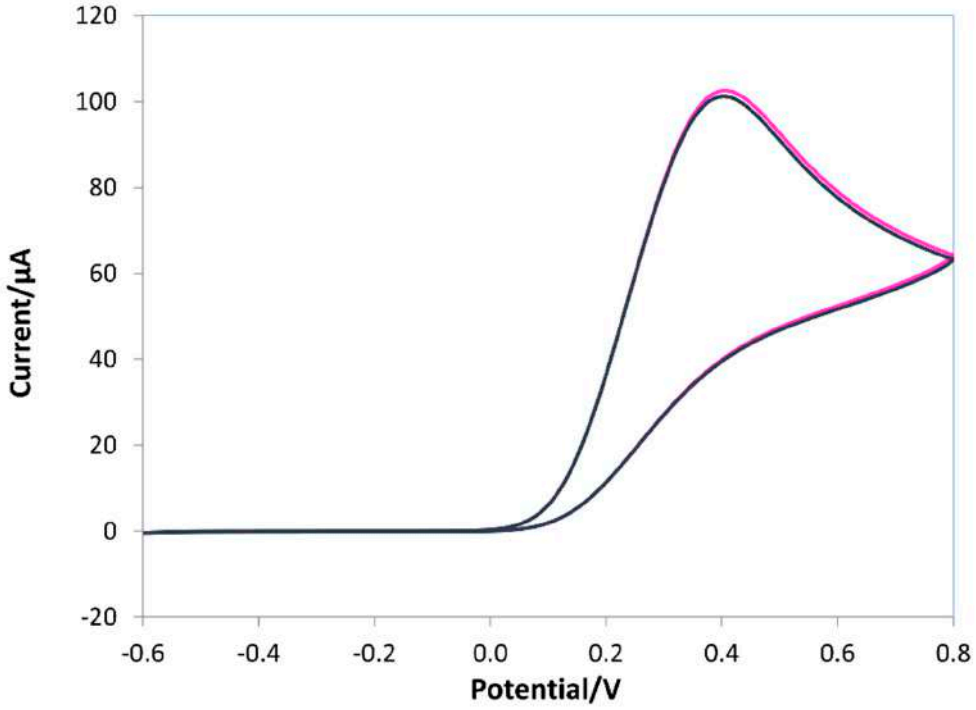

Figure 5. Cyclic voltammograms of 10 mM ascorbic acid in 0.1 M $LiClO_4$ solution. Potential range −0.6–0.8 V, scan rate 0.1 V/s.

In the e-MIP, the template molecules are trapped in the polypyrrole matrix thanks to non-covalent interactions, i.e., hydrogen bonds between the carbonyl and hydroxyl groups of the ascorbic acid and the -NH groups of the pyrrole units.

As will be described below, the DPV measurements with the e-MIP thus obtained showed high background noise and a baseline that was not stable. Therefore, overoxidation was carried out by chronoamperometry at 1.2 V for 2 min in 0.1 M $LiClO_4$ solution before the template extraction. Overoxidation leads to ketone groups forming on the polypyrrole backbone and disrupting conjugation but without significant material loss from the electrode surface [74]; moreover, higher film thickness control arises, and the background currents are definitely stable [53,58,59].

Figure 6 shows a schematic representation of a possible interaction mechanism of ascorbic acid and the overoxidate polypyrrole.

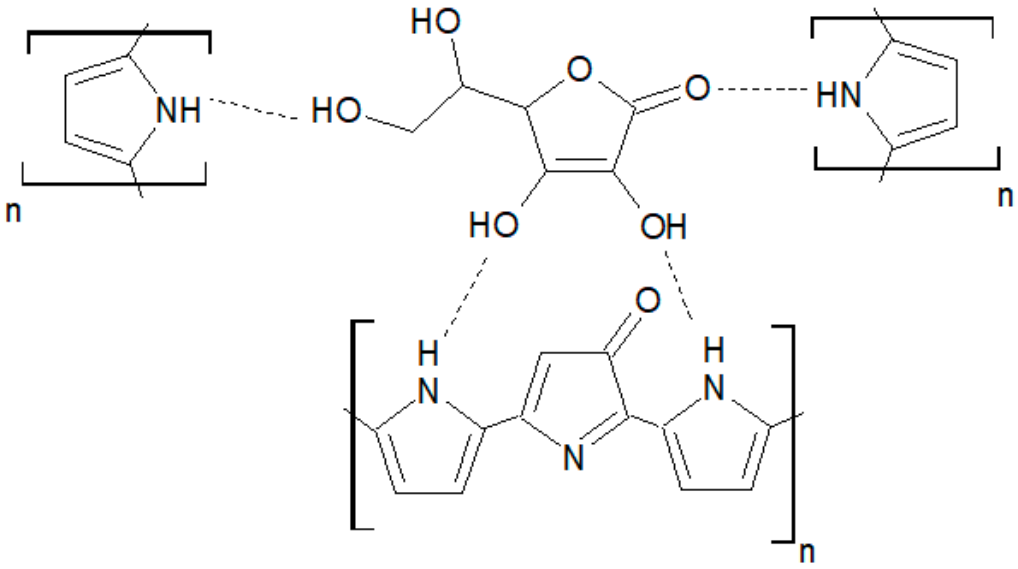

Figure 6. Schematic representation of the interaction mechanism AA/overoxidate polypyrrole.

The extraction of the ascorbic acid molecules from the e-MIP was performed in two steps: washing in PBS solution 0.05 M at pH 7.5 for 20 min, under gentle stirring on an orbital shaker, followed by 10–15 CV scans from −1 to +1 V (scan rate 0.1 V/s) in PBS solution 0.05 M/KCl 0.1 M at pH = 7.5 to remove the entrapped template completely, i.e., until the disappearance of the oxidation peak corresponding to ascorbic acid.

3.4. Electrochemical Detection of Ascorbic Acid: Evaluation of the Analytical Parameters

As stated above, DPV was selected for ascorbic acid detection. Calibration curves were obtained, registering the voltammograms in 10 mL of 0.05 M PBS/0.1 M KCl solutions at pH 7.5 at increasing ascorbic acid concentration and applying the experimental parameters optimized by the DoE approach described in Section 3.1. To compare the analytical figures of merit, bare, e-MIP, and e-NIP electrodes were tested. The voltammograms obtained for the three different electrodes and also the graph for a non-overoxidated e-MIP are reported in Figure 7.

Figure 8 shows the calibration graphs, and Table 6 summarizes the analytical parameters evaluated from the linear regression of the data, i_p (μA) vs. ascorbic acid concentration ([AA]/mM), for the studied electrodes.

Figure 7d shows the voltammograms obtained with the non-overoxidated e-MIP: disturbed signals and high background current are evident, so experiments with this type of modified electrodes have not been continued.

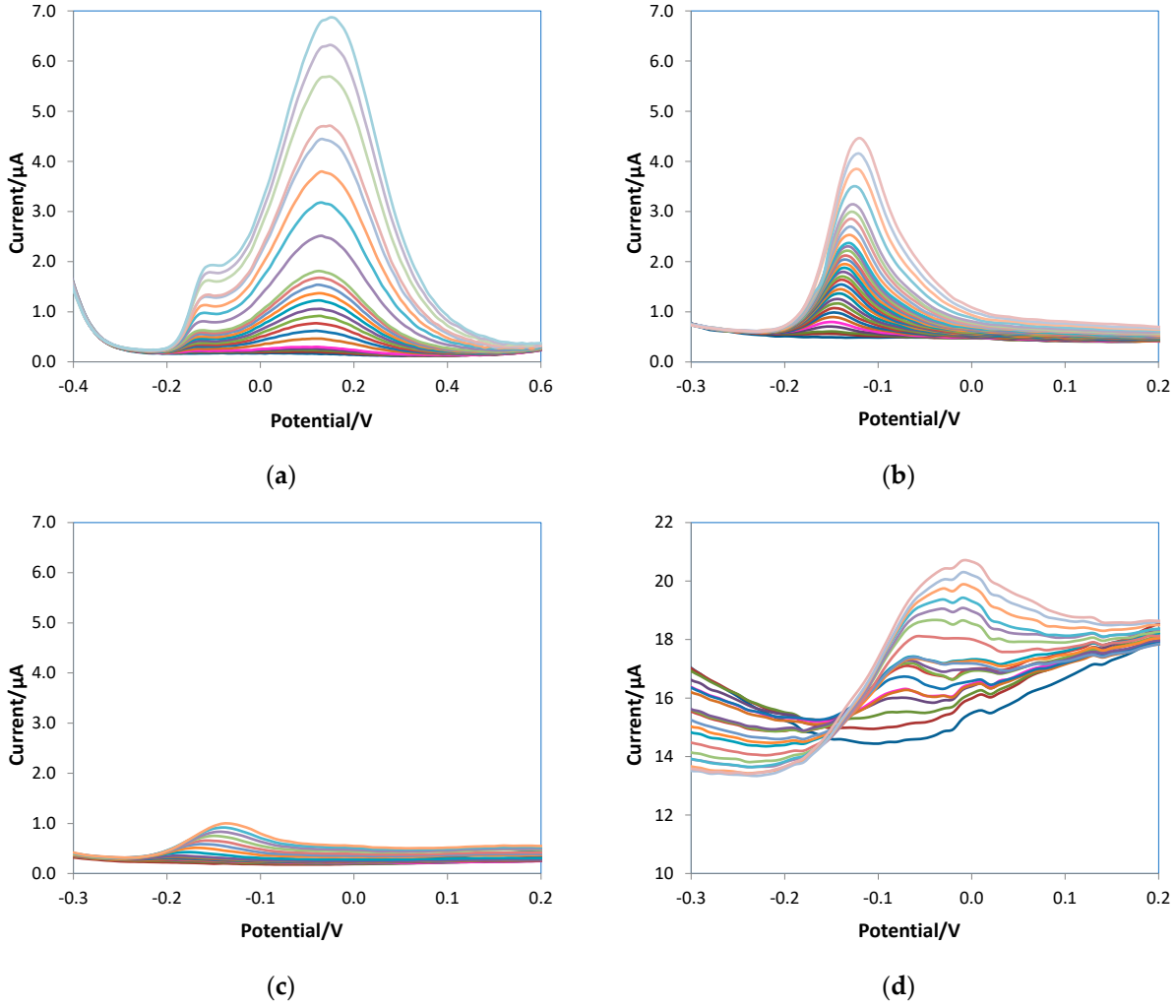

Figure 7. DPV voltammograms of (**a**) bare, (**b**) e-MIP, (**c**) e-NIP, (**d**) non-overoxidate e-MIP registered in 10 mL of 0.05 M PBS/0.1 M KCl solutions at pH 7.5 at increasing ascorbic acid concentration from 0 to 5 mM.

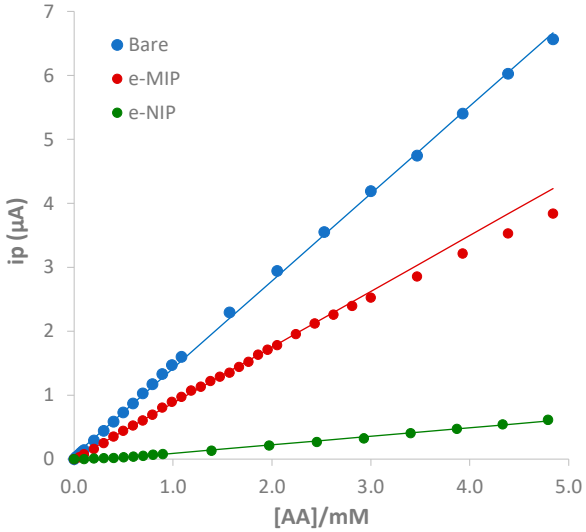

Figure 8. Calibration graphs for bare, e-MIP, and e-NIP obtained, respectively, from the DPV data of Figure 7a–c.

Table 6. Analytical parameters evaluated from the linear regression of the DPV data. Results obtained from three different calibration curves using three screen-printed cells for each type (bare, e-MIP, and e-NIP) in 10 mL of 0.05 M PBS/0.1 M KCl solutions at pH 7.5.

Electrode	Slope (μA mM^{-1})	R^2	LOD [a] (μM)	LOQ (μM)	Linear Range (μM)
bare	1.34(7)	0.999	35	106	20–4800
e-MIP	1.02(6)	0.999	21	64	30–2400
e-MIP [b]	98(2)	0.998	1.2	3.6	2–100
e-NIP	0.13(2)	0.997	150	450	400–4800

[a] LOD = 3.3·$s_{y/x}$/S, where S is the slope of the calibration curve and $s_{y/x}$ is the standard deviation of y-residuals (i.e., the random errors in the y-direction); it can be considered not significantly different from the standard deviation of replicate measurements of blank solutions [75]. The number in parenthesis is the standard deviation of the last digit. [b] calibration in 100 mL of solution.

The slightly higher sensitivity of the bare compared to the overoxidated e-MIP electrode can be immediately noted. However, the linear range, the LOD, and the LOQ are relatively similar, a little better for the e-MIP. Some calibrations were also performed using a ten times higher volume aiming to improve the LOD. A lower detection limit was achieved by applying the same experimental conditions, demonstrating the method's versatility and robustness.

In terms of sensitivity, LOD, and LOQ, it is favorable to obtain parameters similar to the bare electrode for the e-MIP; this means that the polymeric film has a high number of recognition sites for the analyte. The poor sensitivity of the e-NIP is an added advantage since the non-imprinted polymer acts as a barrier to the analyte reaction at the electrode surface (lower electroactive surface available for the analyte oxidation). The preparation of the e-NIP demonstrates the effectiveness and the need for template-driven synthesis for obtaining selective sensors with pretty good sensitivity.

The repeatability of the measurements was also tested. Figure 9 reports the calibration graph of five replicates with the same screen-printed cell. It can be observed that the differences among the replicates are not significant (RDS < 5%).

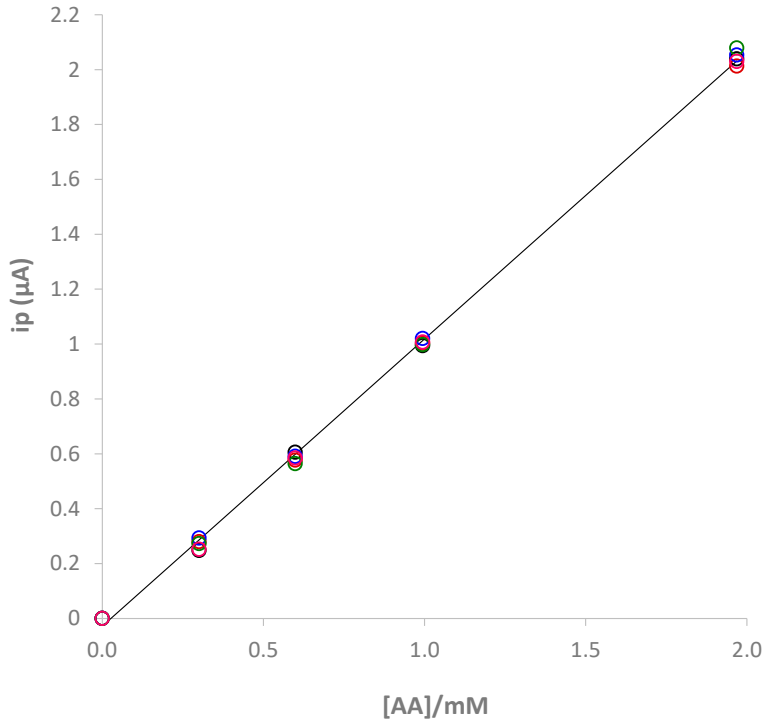

Figure 9. Five replicates of calibration obtained with a single e-MIP-modified screen-printed cell. Data points of each replicate at the same concentration are reported with circles at different color.

3.5. Selectivity Test and Analyses of Commercial Products

The ascorbic acid determination in the presence of two possible interferents, such as dopamine and uric acid, was performed to test the selectivity of the e-MIP electrode. These analytes were selected since their oxidation reactions occur at close potentials [37–39].

Figure 10 shows the voltammograms obtained with the bare electrode. Figure 10a reported the DPVs of 0.5 mM ascorbic acid solutions without and with uric acid additions; as can be observed, the peaks of the two analytes overlap at the lowest uric acid concentration until they merge at higher uric acid additions. Similar behavior occurred when the DPVs were registered in the presence of dopamine as an interferent (Figure 10b).

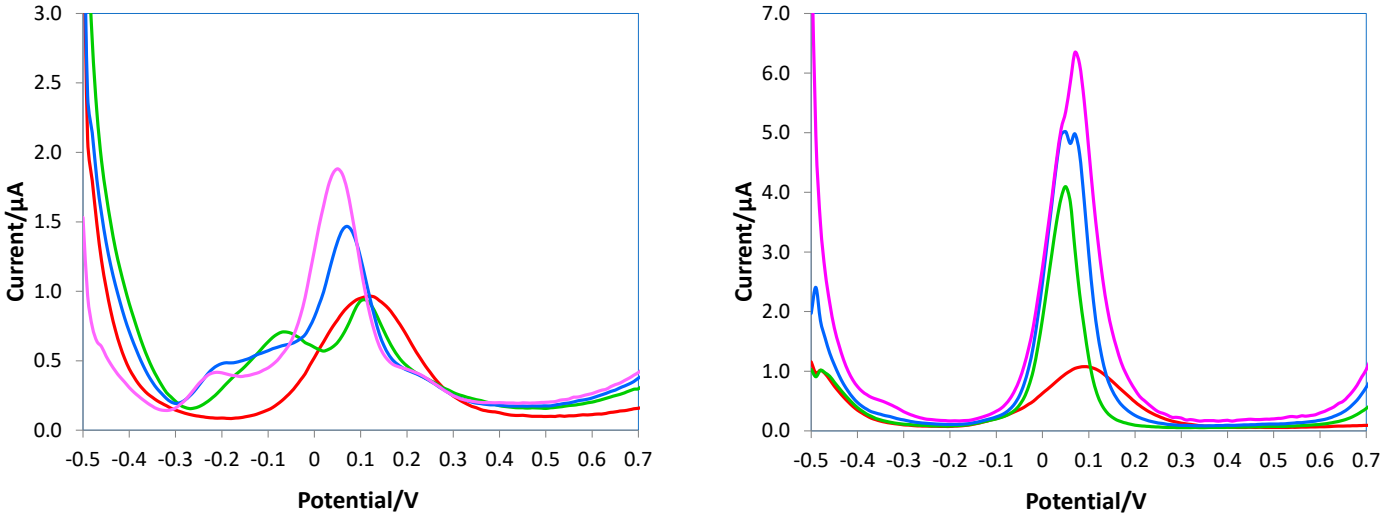

(**a**) (**b**)

Figure 10. DPV voltammograms of the bare electrode registered in 10 mL of 0.05 M PBS/0.1 M KCl solutions at pH 7.5, (**a**) 0.5 mM AA (red line), 0.5 mM AA + 0.3 mM uric acid (green line), 0.5 mM AA + 0.5 mM uric acid (blue line), 0.5 mM AA + 0.8 mM uric acid (pink line); (**b**) 0.5 mM AA (red line), 0.5 mM AA + 0.3 mM dopamine (green line), 0.5 mM AA + 0.5 mM dopamine (blue line), 0.5 mM AA + 0.8 mM dopamine (pink line).

Conversely, the presence of the e-MIP on the electrode surface allows the quantification of the ascorbic acid without interference problems, as can be seen in the voltammograms of Figure 11.

In the presence of uric acid, a shift of the oxidation peak of the ascorbic acid towards less-positive potentials occurred, but the signals of the two analytes are distinct and well resolved, as shown in Figure 11a; here, the same uric acid concentration was added to solutions at increasing ascorbic acid content. Figure 11b shows the distinct signals of ascorbic acid and dopamine, and although there is higher sensitivity for dopamine, the peak high of ascorbic acid does not decrease with the increase in the interferent content.

These results corroborate that the e-MIP-based electrode can selectively recognize ascorbic acid molecules better than the bare one; moreover, with the e-MIP-modified electrode, the simultaneous quantification of the AA, dopamine, and uric acid can be possible since the corresponding DPV peaks do not overlap.

To assess the reliability of the proposed method, two different drug tables with known ascorbic acid content were analyzed. The standard additions method was applied. The results are summarized in Table 7.

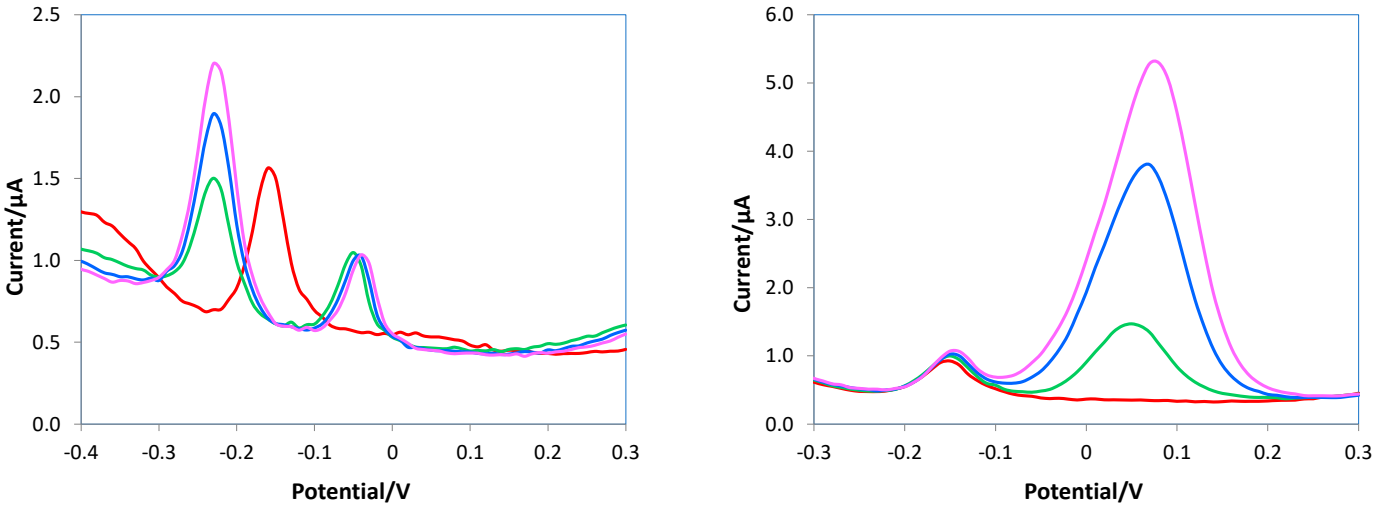

Figure 11. DPV voltammograms of the e-MIP electrode registered in 10 mL of 0.05 M PBS/0.1 M KCl solutions at pH 7.5, (**a**) 1 mM AA (red line), 1 mM AA + 0.4 mM uric acid (green line), 1.2 mM AA + 0.4 mM uric acid (blue line), 1.5 mM AA + 0.4 mM uric acid (pink line); (**b**) 1 mM AA (red line), 1 mM AA + 0.1 mM dopamine (green line), 1 mM AA + 0.2 mM dopamine (blue line), 1 mM AA + 0.3 mM dopamine (pink line).

Table 7. Ascorbic acid detection in farmaceutical products. CI = confidence interval at 95% confidence level. Three replicates for each sample using the same e-MIP screen-printed cell.

	VIVIN C® AA Content (mg)	**TIOBEC® 400 AA Content (mg)**
Average (n = 3)	210	30
Standard deviation	5	2
Upper bound CI	222	35
Lower bound CI	197	24
Declared content	**200**	**30**

For both products, the results obtained are in good agreement with the declared ascorbic acid content; moreover, the low standard deviation reveals a significant reproducibility of the measurements, considering that the same e-MIP-based screen-printed cell was used for both determinations.

4. Conclusions

A molecularly imprinted electrosynthesized polymer (e-MIP) on screen-printed electrodes for ascorbic acid detection by the DPV method was developed.

The best results were obtained after polypyrrole overoxidation, performing the measurements in phosphate buffer solution 0.05 M/KCl 0.1 M at pH 7.5 and applying optimized experimental conditions for the voltammetric detection.

The graphite working electrode surface was characterized before and after modification, measuring the active area and the double-layer capacitance. The results of both determinations demonstrated the electrode surface coverage by the e-MIP layer.

The analytical parameters evaluated from the calibration curves demonstrated good sensitivity and a detection limit not significantly different from that achievable with the non-modified electrode (bare) and similar electrochemical sensors (see Table 1). The LOD obtained is about 20 µM if the sample volume is 10 mL, but the value can be reduced if a higher sample volume is analyzed (e.g.,1.2 µM if the sample volume is 100 mL).

Selectivity tests were undertaken considering dopamine and uric acid as interferents, proving the possibility for the e-MIP-based electrode to quantify ascorbic acid without interference problems or to determine the three analytes simultaneously if all are present in the same sample.

To assess the proposed method's reliability, two pharmaceutical products with known ascorbic acid content were analyzed, and the results obtained agreed with the declared ascorbic acid content.

Although the proposed sensor may seem scarcely sensitive, it is worth noting that ascorbic acid is not a pollutant; moreover, in foods or drugs and even when added as a preservative to avoid the oxidation of foods, it is present at very high concentrations. The scope of this work is to propose a selective method that can detect ascorbic acid directly in a sample without lengthy pretreatment or various dilution steps, using a quick and simple modification of the electrode surface and low-cost and portable apparatus, and is helpful for routine or in situ analyses.

Author Contributions: Conceptualization, G.A.; methodology, C.Z. and G.A.; formal analysis, G.A. and L.R.M.; investigation, G.A. and C.Z.; data curation, L.R.M. and R.B.; writing—original draft preparation, G.A.; writing—review and editing, C.Z., L.R.M. and R.B. All authors have read and agreed to the published version of the manuscript.

Funding: This research received no external funding.

Institutional Review Board Statement: Not applicable.

Informed Consent Statement: Not applicable.

Data Availability Statement: Not applicable.

Acknowledgments: We thank Topflight Italia (S.P.A.) for providing us with screen-printed cells free of charge.

Conflicts of Interest: The authors declare no conflict of interest.

References

1. Pisoschi, A.M.; Pop, A.; Serban, A.I.; Fafaneata, C.H. Electrochemical methods for ascorbic acid determination. *Electrochim. Acta* **2014**, *121*, 443–460.
2. Cathcart, R.F. A unique function for ascorbate. *Med. Hypotheses* **1991**, *35*, 32–37. [CrossRef] [PubMed]
3. Sies, H.; Stahl, W.; Sundquist, A.R. Antioxidant functions of vitamins: Vitamins E and C, Beta-Carotene, and other carotenoids. *Ann. N. Y. Acad. Sci.* **1992**, *669*, 7–20. [CrossRef] [PubMed]
4. Padayatty, S.J.; Katz, A.; Wang, Y.; Eck, P.; Kwon, O.; Lee, J.-H.; Chen, S.; Corpe, C.; Dutta, A.; Dutta, S.K.; et al. Vitamin, C as an antioxidant: Evaluation of its role in disease prevention. *J. Am. Coll. Nutr.* **2003**, *22*, 18–35. [CrossRef]
5. Popa, C.V.; Danet, A.F.; Jipa, S.; Zaharescu, T. Determination of total antioxidant activity of wines using a flow injection method with chemiluminescence detection. *Rev. Chim.* **2010**, *61*, 11–16.
6. Pisoschi, A.M.; Cheregi, M.C.; Danet, A.F. Total Antioxidant Capacity of Some Commercial Fruit Juices: Electrochemical and Spectrophotometrical Approaches. *Molecules* **2009**, *14*, 480–493. [CrossRef]
7. Bradshaw, M.P.; Barril, C.; Clark, A.C.; Prenzler, P.D.; Scollary, G.R. Ascorbic acid: A review of its chemistry and reactivity in relation to a wine environment. *Crit. Rev. Food Sci. Nutr.* **2011**, *51*, 479–498. [CrossRef]
8. Hsu, P.F.; Ciou, W.L.; Chen, P.Y. Voltammetric study of polyviologen and the application of polyviologen-modified glassy carbon electrode in amperometric detection of vitamin C. *J. Appl. Electrochem.* **2008**, *38*, 1285–1292. [CrossRef]
9. Deshmukh, G.S.; Bapat, M.G. Determination of ascorbic acid by potassium iodate. *Fresenius Z. Anal. Chem.* **1955**, *145*, 254–256. [CrossRef]
10. McHenry, E.W.; Graham, M. Observations on the estimation of ascorbic acid by titration. *Biochem. J.* **1935**, *29*, 2013–2019. [CrossRef]
11. Kall, M.A.; Andersen, C. Improved method for simultaneous determination of ascorbic acid and dehydroascorbic acid, isoascorbic acid and dehydroisoascorbic acid in food and biological samples. *J. Chromatogr. B* **1990**, *730*, 101–111. [CrossRef] [PubMed]
12. Iwase, H.; Ono, I. Determination of ascorbic acid in food by column liquid chromatography with electrochemical detection using eluent for pre-run sample stabilization. *J. Chromatogr. B* **1998**, *806*, 361–364. [CrossRef] [PubMed]
13. Iwase, H. Use of nucleic acids in the mobile phase for the determination of ascorbic acid in foods by high-performance liquid chromatography with electrochemical detection. *J. Chromatogr. A* **2000**, *881*, 327–330. [CrossRef] [PubMed]

14. Borowski, J.; Szajdek, A.; Borowska, E.J.; Ciska, E.; Zieliński, H. Content of selected bioactive components and antioxidant properties of broccoli (*Brassica oleracea* L.). *Eur. Food Res. Technol.* **2008**, *226*, 459–465. [CrossRef]
15. Nobrega, J.A.; Lopes, J.S. Flow injection spectrophotometric determination of ascorbic acid in pharmaceutical products with the Prussian Blue reaction. *Talanta* **1996**, *43*, 971–976. [CrossRef]
16. Lenarczuk, T.; Głab, S.; Koncki, R. Application of Prussian blue-based optical sensor in pharmaceutical analysis. *J. Pharm. Biomed. Anal.* **2001**, *26*, 163–169. [CrossRef]
17. Güçlü, K.; Sözgen, K.; Tütem, E.; Özyürek, M.; Apak, R. Spectrophotometric determination of ascorbic acid using copper(II)-neocuproine reagent in beverages and pharmaceuticals. *Talanta* **2005**, *65*, 1226–1232. [CrossRef]
18. Vermeir, S.; Hertog, M.L.A.T.M.; Schenk, A.; Beullens, K.; Nicolai, B.M.; Lammertyn, J. Evaluation and optimization of high-throughput enzymatic assays for fast l-ascorbic acid quantification in fruit and vegetables. *Anal. Chim. Acta* **2008**, *618*, 94–101. [CrossRef]
19. Wawrzyniak, J.; Ryniecki, A.; Zembrzuski, W. Application of voltammetry to determine vitamin C in apple juices. *Acta Sci. Pol. Technol. Aliment.* **2005**, *42*, 5–16.
20. Nezamzadeh, A.; Amini, M.K.; Faghihian, H. Square-wave voltammetric determination of ascorbic acid based on its electrocatalytic oxidation at zeolite-modified carbon-paste electrodes. *Int. J. Electrochem. Sci.* **2007**, *2*, 583–594.
21. Raoof, J.B.; Ojani, R.; Beitollahi, H. Electrocatalytic determination af ascorbic acid at chemically modified carbon paste electrode with 2,7 bis(ferrocenyl ethynyl) fluoren-9-one. *Int. J. Electrochem. Sci.* **2007**, *2*, 534–548.
22. Ensafi, A.A.; Taei, M.; Khayamian, T. A differential pulse voltammetric method for simultaneous determination of ascorbic acid, dopamine and uric acid using poly(3-(5-chloro-2-hydroxyphenylazo)-4,5-dihydroxynaphtalene-2,7-disulphonic acid) film modified glassy carbon electrode. *J. Electroanal. Chem.* **2009**, *633*, 212–220. [CrossRef]
23. Dechakiatkrai, C.; Chen, J.; Lynam, C.; Shin, K.M.; Kim, S.J.; Phanichphant, S.; Wallace, G.G. Direct Ascorbic Acid Detection with Ferritin Immobilized on Single-Walled Carbon Nanotubes. *Electrochem. Solid-State Lett.* **2008**, *11*, 4–6. [CrossRef]
24. Li, F.; Tang, C.; Liu, S.; Ma, G. Development of an electrochemical ascorbic acid sensor based on the incorporation of a ferricyanide mediator with a polyelectrolyte–calcium carbonate microsphere. *Electrochim. Acta* **2010**, *55*, 838–843. [CrossRef]
25. Pisoschi, A.M.; Pop, A.; Negulescu, G.P.; Pisoschi, A. Determination of Ascorbic Acid Content of Some Fruit Juices and Wine by Voltammetry Performed at Pt and Carbon Paste Electrodes. *Molecules* **2011**, *16*, 1349–1365. [CrossRef]
26. Li, F.; Li, J.; Feng, Y.; Yang, L.; Du, Z. Electrochemical behavior of graphene doped carbon paste electrode and its application for sensitive determination of ascorbic acid. *Sens. Actuators B Chem.* **2011**, *157*, 110–114. [CrossRef]
27. Shankar, S.S.; Swamy, B.K.; Chandrashekar, B.N.; Gururaj, K.J. Sodium dodecyl benzene sulfate modified carbon paste electrode as an electrochemical sensor for the simultaneous analysis of dopamine, ascorbic acid and uric acid: A voltammetric study. *J. Mol. Liq.* **2013**, *177*, 32–39. [CrossRef]
28. Hu, I.; Kuwana, T. Oxidative mechanism of ascorbic acid at glassy carbon electrodes. *Anal. Chem.* **1986**, *58*, 3235–3239. [CrossRef]
29. Rueda, M.; Aldaz, A.; Sanchez-Burgos, F. Oxidation of L-ascorbic acid on a gold electrode. *Electrochim. Acta* **1978**, *23*, 419–424. [CrossRef]
30. Chen, Z.; Zu, Y. Simultaneous detection of ascorbic acid and uric acid using a fluorosurfactant modified platinum electrode. *J. Electroanal. Chem.* **2007**, *603*, 281–286. [CrossRef]
31. Zare, H.R.; Memarzadeh, F.; Mazloum Ardakani, M.; Namazian, M.; Golabi, S.M. Norepinephrine-modified glassy carbon electrode for the simultaneous determination of ascorbic acid and uric acid. *Electrochim. Acta* **2005**, *50*, 3495–3502. [CrossRef]
32. Lin, X.; Li, Y. Monolayer covalent modification of 5-hydroxytryptophan on glassy carbon electrodes for simultaneous determination of uric acid and ascorbic acid. *Electrochim. Acta* **2006**, *51*, 5794–5801. [CrossRef]
33. Hu, G.; Ma, Y.; Guo, Y.; Shao, S. Electrocatalytic oxidation and simultaneous determination of uric acid and ascorbic acid on the gold nanoparticles modified glassy carbon electrode. *Electrochim. Acta* **2008**, *53*, 6610–6615. [CrossRef]
34. Gupta, V.K.; Jain, A.K.; Shoora, S.K. Multiwall carbon nanotube modified glassy carbon electrode as voltammetric sensor for the simultaneous determination of ascorbic acid and caffeine. *Electrochim. Acta* **2013**, *93*, 248–253. [CrossRef]
35. Raoof, J.B.; Kiani, A.; Ojani, R.; Valiollahi, R.; Rashid-Nadimi, S. Simultaneous voltammetric determination of ascorbic acid and dopamine at the surface of electrodes modified with self-assembled gold nanoparticle films. *J. Solid State Electrochem.* **2010**, *14*, 1171–1176. [CrossRef]
36. Jilani, B.S.; Pari, M.; Reddy, K.V.; Lokesh, K.S. Simultaneous and sensitive detection of ascorbic acid in presence of dopamine using MWCNTs-decorated cobalt (II) phthalocyanine modified GCE. *Microchem. J.* **2019**, *147*, 755–763.
37. Tonelli, D.; Ballarin, B.; Guadagnini, L.; Mignani, A.; Scavetta, E. A novel potentiometric sensor for l-ascorbic acid based on molecularly imprinted polypyrrole. *Electrochim. Acta* **2011**, *56*, 7149–7154. [CrossRef]
38. Yan, C.; Liu, X.; Zhang, R.; Chen, Y.; Wang, G. A selective strategy for determination of ascorbic acid based on molecular imprinted copolymer of o-phenylenediamine and pyrrole. *J. Electroanal. Chem.* **2016**, *780*, 276–281. [CrossRef]
39. Özcan, L.; Sahin, M.; Sahin, Y. Electrochemical Preparation of a Molecularly Imprinted Polypyrrole-modified Pencil Graphite Electrode for Determination of Ascorbic Acid. *Sensors* **2008**, *8*, 5792–5805. [CrossRef]
40. Oliveira, S.M.; Luzardo, J.M.; Silva, L.A.; Aguiar, D.; Senna, C.; Verdan, R.; Kuznetsov, A.; Vasconcelos, T.; Archanjo, B.; Achete, C.; et al. High-performance electrochemical sensor based on molecularly imprinted polypyrrole-graphene modified glassy carbon electrode. *Thin Solid Films* **2020**, *699*, 137875. [CrossRef]

41. Blanco-López, M.C.; Gutiérrez-Fernández, S.; Lobo-Castañón, M.J.; Miranda-Ordieres, A.J.; Tuñón-Blanco, P. Electrochemical sensing with electrodes modified with molecularly imprinted polymer films. *Anal. Bioanal. Chem.* **2004**, *378*, 1922–1928. [CrossRef] [PubMed]
42. Merkoci, A.; Alegret, S. New materials for electrochemical sensing IV. Molecular imprinted polymers. *TrAC Trends Anal. Chem.* **2002**, *21*, 717–725. [CrossRef]
43. Leibl, N.; Haupt, K.; Gonzato, C.; Duma, L. Molecularly Imprinted Polymers for Chemical Sensing: A Tutorial Review. *Chemosensors* **2021**, *9*, 123. [CrossRef]
44. Rebelo, P.; Costa-Rama, E.; Seguro, I.; Pacheco, J.G.; Nouws, H.P.; Cordeiro, M.N.D.; Delerue-Matos, C. Molecularly imprinted polymer-based electrochemical sensors for environmental analysis. *Biosens. Bioelectron.* **2021**, *172*, 112719. [CrossRef] [PubMed]
45. Scheller, F.W.; Zhang, X.; Yarman, A.; Wollenberger, U.; Gyurcsányi, R.E. Molecularly imprinted polymer-based electrochemical sensors for biopolymers. *Curr. Opin. Electrochem.* **2009**, *14*, 53–59. [CrossRef]
46. Ayerdurai, V.; Cieplak, M.; Kutner, W. Molecularly imprinted polymer-based electrochemical sensors for food contaminants determination. *TrAC Trends Anal. Chem.* **2022**, *158*, 116830. [CrossRef]
47. Shah, N.S.; Thotathil, V.; Zaidi, S.A.; Sheikh, H.; Mohamed, M.; Qureshi, A.; Sadasivuni, K.K. Picomolar or beyond Limit of Detection Using Molecularly Imprinted Polymer-Based Electrochemical Sensors: A Review. *Biosensors* **2022**, *12*, 1107. [CrossRef]
48. Zheng, X.; Khaoulani, S.; Ktari, N.; Lo, M.; Khalil, A.M.; Zerrouki, C.; Fourati, N.; Chehimi, M.M. Towards Clean and Safe Water: A Review on the Emerging Role of Imprinted Polymer-Based Electrochemical Sensors. *Sensors* **2021**, *21*, 4300. [CrossRef]
49. Ramanavicius, S.; Samukaite-Bubniene, U.; Ratautaite, V.; Bechelany, M.; Ramanavicius, A. Electrochemical molecularly imprinted polymer based sensors for pharmaceutical and biomedical applications. *J. Pharm. Biomed. Anal.* **2022**, *215*, 114739. [CrossRef]
50. Akgönüllü, S.; Kılıç, S.; Esen, C.; Denizli, A. Molecularly Imprinted Polymer-Based Sensors for Protein Detection. *Polymers* **2023**, *15*, 629. [CrossRef]
51. Mazzotta, E.; Di Giulio, T.; Malitesta, C. Electrochemical sensing of macromolecules based on molecularly imprinted polymers: Challenges, successful strategies, and opportunities. *Anal. Bioanal. Chem.* **2022**, *414*, 5165–5200. [CrossRef] [PubMed]
52. Gonçalves, L.M. Electropolymerized molecularly imprinted polymers: Perceptions based on recent literature for soon-to-be world-class scientists. *Curr. Opin. Electrochem.* **2021**, *25*, 100640. [CrossRef]
53. Crapnell, R.D.; Hudson, A.; Foster, C.W.; Eersels, K.; Grinsven, B.v.; Cleij, T.J.; Banks, C.E.; Peeters, M. Recent Advances in Electrosynthesized Molecularly Imprinted Polymer Sensing Platforms for Bioanalyte Detection. *Sensors* **2019**, *19*, 1204. [CrossRef] [PubMed]
54. Unger, C.; Lieberzeit, P.A. Molecularly imprinted thin film surfaces in sensing: Chances and challenges. *React. Funct. Polym.* **2021**, *161*, 104855.
55. Ramanavicius, S.; Ramanavicius, A. Charge Transfer and Biocompatibility Aspects in Conducting Polymer-Based Enzymatic Biosensors and Biofuel Cells. *Nanomaterials* **2021**, *11*, 371. [CrossRef]
56. Ramanavičius, S.; Morkvėnaitė-Vilkončienė, I.; Samukaitė-Bubnienė, U.; Ratautaitė, V.; Plikusienė, I.; Viter, R.; Ramanavičius, A. Electrochemically Deposited Molecularly Imprinted Polymer-Based Sensors. *Sensors* **2022**, *22*, 1282. [CrossRef]
57. Sadki, S.; Schottland, P.; Brodie, N.; Sabouraud, G. The mechanisms of pyrrole electropolymerization. *Chem. Soc. Rev.* **2000**, *29*, 12.
58. Witkowski, A.; Freund, M.S.; Brajter-Toth, A. Effect of Electrode Substrate on the Morphology and Selectivity of Overoxidized Polypyrrole Films. *Anal. Chem.* **1991**, *63*, 622–626. [CrossRef]
59. Hsueh, C.; Brajter-Toth, A. Electrochemical Preparation and Analytical Applications of Ultrathin Overoxidized Polypyrrole Films. *Anal. Chem.* **1994**, *66*, 2458–2464. [CrossRef]
60. Burak, D.; Emregul, E.; Emregul, K.C. Copper–zinc alloy nanoparticle based enzyme-free superoxide radical sensing on a screen-printed electrode. *Talanta* **2015**, *134*, 206–214.
61. Pesavento, M.; Merli, D.; Biesuz, R.; Alberti, G.; Marchetti, S.; Milanese, C. A MIP-based low-cost electrochemical sensor for 2-furaldehyde detection in beverages. *Anal. Chim. Acta* **2021**, *1142*, 201–210. [CrossRef]
62. Pesavento, M.; D'agostino, G.; Alberti, G.; Biesuz, R.; Merli, D. Voltammetric platform for detection of 2,4,6-trinitrotoluene based on a molecularly imprinted polymer. *Anal. Bioanal. Chem.* **2013**, *405*, 3559–3570. [CrossRef] [PubMed]
63. Akhoundian, M.; Alizadeh, T.; Ganjali, M.R.; Rafiei, F. A new carbon paste electrode modified with MWCNTs and nano-structured molecularly imprinted polymer for ultratrace determination of trimipramine: The crucial effect of electrode components mixing on its performance. *Biosens. Bioelectron.* **2018**, *111*, 27–33. [CrossRef] [PubMed]
64. Magar, H.S.; Hassan, R.Y.A.; Mulchandani, A. Electrochemical Impedance Spectroscopy (EIS): Principles, Construction, and Biosensing Applications. *Sensors* **2021**, *21*, 6578. [CrossRef]
65. Craven, J.E.; Kinnamon, D.S.; Prasad, S. Randles Circuit Analysis Toward Investigating Interfacial Effects on Microchannel Electrodes. *IEEE Sens. Lett.* **2018**, *2*, 15–18. [CrossRef]
66. Chemometric Agile Tool (CAT). Available online: http://www.gruppochemiometria.it/index.php/software/19-download-therbased-chemometric-software (accessed on 3 April 2023).
67. Banks, C.E.; Compton, R.G. New electrodes for old: From carbon nanotubes to edge plane pyrolytic graphite. *Analyst* **2006**, *131*, 15–21. [CrossRef]
68. Maouche, N.; Guergouri, M.; Gam-Derouich, S.; Jouini, M.; Nessark, B.; Chehimi, M.M. Molecularly imprinted polypyrrole films: Some key parameters for electrochemical picomolar detection of dopamine. *J. Electroanal. Chem.* **2012**, *685*, 21–27. [CrossRef]

69. Radi, A.E.; El-Naggar, A.E.; Nassef, H.M. Determination of coccidiostat clopidol on an electropolymerized-molecularly imprinted polypyrrole polymer modified screen printed carbon electrode. *Anal. Meth.* **2014**, *6*, 7967–7972. [CrossRef]
70. Ozkorucuklu, S.P.; Sahin, Y.; Alsancak, G. Voltammetric Behaviour of Sulfamethoxazole on Electropolymerized-Molecularly Imprinted Overoxidized Polypyrrole. *Sensors* **2008**, *8*, 8463–8478. [CrossRef]
71. Nezhadali, A.; Mojarrab, M. Computational study and multivariate optimization of hydrochlorothiazide analysis using molecularly imprinted polymer electrochemical sensor based on carbon nanotube/polypyrrole film. *Sens. Actuators B Chem.* **2014**, *190*, 829–837. [CrossRef]
72. Devkota, L.; Nguyen, L.T.; Vu, T.T.; Piro, B. Electrochemical determination of tetracycline using AuNP-coated molecularly imprinted overoxidized polypyrrole sensing interface. *Electrochim. Acta* **2018**, *270*, 535–542. [CrossRef]
73. Pour, B.H.; Haghnazari, N.; Keshavarzi, F.; Ahmadi, E.; Zarif, B.R. A sensitive sensor based on molecularly imprinted polypyrrole on reduced graphene oxide modified glassy carbon electrode for nevirapine analysis. *Anal. Meth.* **2021**, *13*, 4767–4777. [CrossRef] [PubMed]
74. Christensen, P.A.; Hamnett, A. In situ spectroscopic investigations of the growth, electrochemical cycling and overoxidation of polypyrrole in aqueous solution. *Electrochim. Acta* **1991**, *36*, 1263–1286. [CrossRef]
75. Miller, J.N.; Miller, J.C. Calibration methods in instrumental analysis: Regression and correlation. In *Statistics and Chemometrics for Analytical Chemistry*, 6th ed.; Pearson Education Limited: Harlow, UK, 2010; pp. 124–126.